Scientific Research Publishing

Engineering, 2023, 15, 24-46
https://www.scirp.org/journal/eng
ISSN Online: 1947-394X
ISSN Print: 1947-3931

High-Inclination Coring of Chang-6_3 of the Yanchang Formation in Huaqing Oilfield, Ordos Basin: Implications for Ancient Flow Direction and Fracture Orientation

Kun Chen[1], Xuefeng Qü[1], Qichao Xie[1], Jian Liu[1], Jiwei Wang[1], Youan He[1], Dong Sun[1], Yexiong Peng[2]

[1]Research Institute of Exploration and Development, PetroChina Changqing Oilfield Company, Xi'an, China
[2]No. 10 Oil Production Plant, PetroChina Changqing Oilfield Company, Qingyang, China
Email: 489517116@qq.com, qxf_cq@petrochina.com.cn, xqc_cq@petrochina.com.cn, liuj2011_cq@petrochina.com.cn, wangjw_cq@petrochina.com.cn, hya_cq@petrochina.com.cn, sd_cq@petrochina.com.cn, pengyx_cq@petrochina.com.cn

How to cite this paper: Chen, K., Qü, X.F., Xie, Q.C., Liu, J., Wang, J.W., He, Y.A., Sun, D. and Peng, Y.X. (2023) High-Inclination Coring of Chang-6_3 of the Yanchang Formation in Huaqing Oilfield, Ordos Basin: Implications for Ancient Flow Direction and Fracture Orientation. *Engineering*, **15**, 24-46.
https://doi.org/10.4236/eng.2023.151003

Received: December 15, 2022
Accepted: January 28, 2023
Published: January 31, 2023

Abstract

A promising method is to use coring of high-inclination well to find ancient flow direction and orient tiny natural fractures in massive sandstone of sandy debris flow. Determination of ancient flow direction can reduce the number of exploration wells, and orientation of natural fractures is of guiding significance to the deployment of water injection development well pattern. In Block X of Huaqing Oilfield, Ordos Basin, the cores of Chang 6_3 section were obtained from Well Y through 16 coring operations, with a total length of 105 m. Cores is oriented through drilling parameters, the number of cores, the angle between the core edge and horizontal bedding, the coincidence degree of core profile and directional flame structure. Therefore, the micro-fractures on the core are directional. The ancient flow directions of sandy debris flow were restored by load casting, groove casting, groove casting and imbricate structure. Our results show that the ancient flow directions of sandy debris flows were southwest, southeast, northwest, and west from bottom to top. The front of the Wuqi Delta is the main source of blocky sandstone with the best oil-bearing property. Affected by the topography of the lake bottom, the sandy debris flow turned locally in the northeast direction, and the sandy debris flow from this direction was formed. The NEE-SWW-trending fractures formed in the Yanshanian period are most developed in the Huaqing area, which should be considered in deploying the flooding well network. The north-south micro-fractures formed in the Himalayan period can improve the physical properties of tight sandstone, which is of great significance for tight sandstone reservoirs.

Keywords

Core Orientation, Tight Sandstone Reservoirs, Sandy Debris Flow

1. Introduction

Typical thick fine sandstone reservoirs related to gravity flow and deep water traction current are developed in the Yanchang Formation of Huaqing Oilfield, Ordos Basin [1]. The gravity flow can be divided into five types: slump, sandy debris flow, turbidite, delta sandstone and underflow transforming sandstone [2] [3]. The gravity sandstone extends in semi-deep lake and deep lake mudstone, and is laterally connected with Chang 7 source rock, which develops favorable reservoir-forming combination [4]-[10]. Even sandstones with poor physical properties become oil-rich due to strong hydrocarbon injection. Among them, the massive sandstone of sandy debris flows in the Chang-6_3 layer in the Chang-6 Member of the Yanchang Formation is the most promising target in the exploration of gravity flow reservoirs, which is the thickest with the best oil-bearing property [11] [12].

Oil companies have successively discovered that deep-water sedimentary gravity flow sandstone reservoirs are related to sandy debris flow with abundant oil content. However, reservoir prediction is the key to exploring and developing these reservoirs [4]. Due to the lack of research on the propagation law of sandy debris flow, it is still complicated matter to predict the distribution direction of sandy debris flow at present. The sedimentary process in the deep-water environment is challenging to observe. Deep-water gravity flow sedimentary microfacies and distribution law of sandstone have not been recognized consistently. Exploring deep-water gravity flow tight oil and gas still has the following problems [13]:

1) The interpretation of reservoir origin is confused.

2) The predictive geological model is missing.

3) Understanding the transport, sedimentary mechanism, and development model of underwater debris flow is low.

It seems feasible to seek the massive sandstone along the provenance direction of sandy debris flows. Provenance direction is often roughly determined by light and heavy mineral analysis [14] [15] [16] [17] and sand composition analysis [2] [18] based on cores from hundreds of wells and dozens of profiles. Even so, up to now, many studies have shown that multiple provenance directions in Huaqing Oilfield. The research results of contributions made by different provenance are also ambiguous. Luo *et al.* [14] showed main provenances from the southwest, northwest, and southeast, and subordinate provenances from the northeast and east in the southwestern Ordos basin. However, several lines of evidence suggest that provenance supply was mainly from the north and northeast directions, and the north direction is the main [15] [16]. Liao *et al.* [17] demonstrated

two provenances in northeast and southwest directions because there is a noticeable difference in quartz and feldspar content between southwest provenance and northeast provenance. Fu *et al.* [2] found that Well Zhuang 61 in the northeast of Huaqing Oilfield had typical mixed provenance characteristics according to the content of quartz and feldspar. That is, there must be southwest provenance in Huaqing Oilfield. Liao *et al.* [19] compared lithofacies differences and claimed that the sandy debris flows sediment developed in the deep-water area in front of the north-east delta from the meandering river. The turbidite mainly developed in the deep-water area of the braided river delta, whose provenance came from the west, southwest, and south. Li *et al.* (2019) [20] thought that provenances of the northeast and east were significantly strengthened during this period.

In addition, the ancient flow direction of sandy debris flows in the Huaqing area is often inconsistent with the provenance direction due to the variability of lake bottom topography. Therefore, the guiding significance of provenance direction for the oilfield exploration and scrolling development of small area X block in Huaqing Oilfield is limited. Predicting the ancient flow direction of sandy debris flows in a small range on sandstone distribution direction is more reliable. It is urgent to reconstruct the ancient flow direction of channel sandy debris in a relatively small oilfield and predict massive fine sandstone distribution direction. This problem restricts the rolling exploration of the oilfield and affects the probability of horizontal well drilling encountering sandstone reservoirs.

In addition to the research on the spreading direction of massive sandstone, the fracture orienting of massive sandstone is of interest because it determines the deployment of the flooding well network. Most researchers investigating the trend of fractures have utilized imaging logging and outcrop measured data [21] [22] [23] [24] [25]. Su *et al.* (2017) [26] have utilized production performance analysis and numerical simulation. In addition, 3D seismic data and seismic anisotropy analysis were sometimes combined with imaging logging to orient fractures [27] [28]. Several systematic, comprehensive analysis methods of these data have been undertaken, such as the statistics method [29], rescaled range analysis method [30], and finite difference method [31]. However, the validity of the analogy is often questioned as, in most cases, the outcrops at the edge of the basin are usually far from the study area in the center of the basin. Besides, large fractures can be identified by logging and seismic, but natural micro-fractures in tight sandstone reservoirs are challenging to identify. Complex statistical methods could not improve the accuracy of the original data as well.

Core data is the most reliable data in the study of ancient flow direction and fracture orientation. Many imbricate structures, load casts, flute casts, and groove casts have been found in the vertical coring of the Yanchang Formation in the Huaqing area. However, these directional bedding structures and bedding plane structures were only used as sedimentary facies symbols due to the lack of core

orientation [12] [32] [33] [34] [35]. In fracture orientation, core data with higher fracture resolution are only a supplement to logging data and outcrop data. Thus, more detailed fracture characterization and paleocurrent evidence can be provided if the core could be oriented.

Traditionally, the core orientation has been assessed by oriented sampling, which indicates direction by side face notch, end face drilling, and directional print. There are specific problems with the use of oriented sampling. One of these is that directional marking of a core surface is not clear when the core is too hard. One of these is that the coring machine is complex, bulky, and expensive, and it is easy to cause hole wall collapse. The directional effect is poor when the drilling top angle is less than 5˚. In addition, research on residual magnetism of the clastic rock has been done to reset the core [36] [37]. However, the measuring accuracy of reduction magnetism is affected by the content of hematite and magnetite and is also greatly affected by human interference [38].

The high-inclination coring has several attractive features: the issue of unclear or damaged markup does not exist because orientation markup is not required. Cores have more complete bedding plane structures and more extended bedding structures due to the longer horizontal offset. Cores of 3 - 4 times vertical core length can be obtained at the same depth, which can be used for water flooding experiments and seepage experiments, making the experimental conditions closer to the actual formation conditions and having minor errors. The machine needed for coring is consistent with the vertical coring machine, and the difficulty of coring is not significantly increased compared with the ordinary vertical coring.

This paper investigates the usefulness of high-inclination coring and proposes a new research idea for core orientation. The rocks of tight sandstone reservoirs in a deep water environment are very suitable for orientation with high inclination. Ancient flow directions reconstruction of sandy debris flows, which can be used as a reference to the distribution direction of sandstone, and the fracture orientation can be determined after core orientation. As a result, the drilling direction of exploration wells can be more precise, thereby reducing the number of exploration wells; the deployment of injection-production well patterns can be more reasonable to prevent flooding. The findings should make an essential contribution to the exploration and scrolling development of deep-water tight sandstone reservoirs.

2. Geological Setting

Ordos Basin is the second-largest inland basin in China and is located west of the North China Block. During the sedimentary period of the Triassic Yanchang Formation, fluvial, delta, and lacustrine deposits were widely developed in Ordos Basin. The Huaqing area is located in the sedimentary center of the Ordos Basin (**Figure 1(A)**) [39]. The sedimentary evolution of the lake basin experienced the whole process of formation, development, prosperity, decline, and extinction

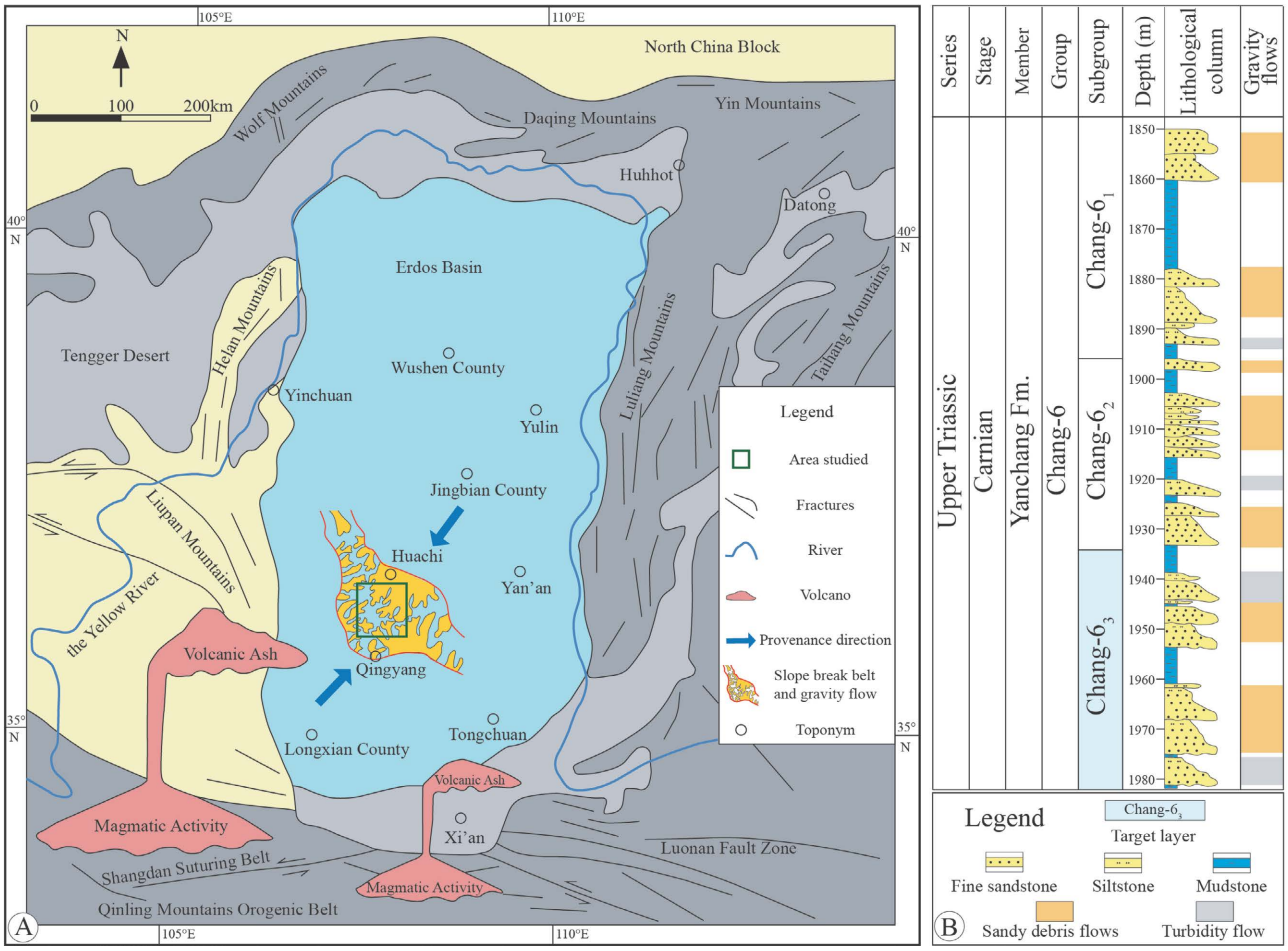

Figure 1. (A) Location map of the Ordos Basin structure and study area (Chen *et al*., 2021). (B) Lithology histogram of Chang-6 of Yanchang Formation in Huaqing area, Ordos Basin (Fu *et al*., 2019).

[1]. Thick deep-water gravity flow sandstone in the middle and lower part of Chang-6 oil formation in Ordos Basin is the direct product of the Middle Indosinian tectonic activity in the Qinling orogenic belt, which caused rapid subsidence of Ordos Basin [40]. The sedimentary period of the Chang-6 Member was mainly in the semi-deep lake and deep lake environment. Previous research has established that the sediment gravity flows of Chang-6 can be divided into sandy debris flows, classic turbidite, and slump [3]. Two major provenance systems from northeast and southwest are intersected in southwestern Huaqing, resulting in inconspicuous differentiation of sedimentary facies in this intersection area [17]. Block X is a major oil-producing area in Huaqing Oilfield. The massive sandstone of the Chang-6_3 layer is the most developed in the Chang-6 Member of the Yanchang Formation (**Figure 1(B)**) [41]. The excellent source-reservoir combination makes the Chang-6_3 layer the most critical exploration target. The number of fracturing segments strictly controls the oil production of Chang-6_3 tight sandstone reservoir in Huaqing Oilfield. In order to have a longer reservoir length so that more crude oil will be produced, high-inclination drilling in massive sandstone is the best choice. High-inclination drilling also creates conditions for

us to use drilling data to orientate the core in the high-inclination section.

3. Materials and Methods

The research data in this paper is drawn from a 105 m long Chang-6_3 core of a high-inclination well Y in Block X of Huaqing Oilfield, Ordos Basin. The drilling deviation of well Y was about 75.6˚ (**Figure 2(A)**), and the azimuth was about 346.5˚, that is, north by west 15˚ (**Figure 2(B)**). In order to identify the spatial relationship of cores, the following parameters were used: dip angle and dip direction of drilling well trajectory, core number, coincidence degree of core cross-section, bedding plane structures, and bedding structures. Just as the gyroscope determines the orientation through two rotors, the orientation of the core can be reset through the rotating coring tube and a virtual rotor which consists of horizontal stratification and flame structure (**Figure 2(C)**).

The determination of core top and bottom can be based on the following five criteria (**Figure 3**):

1) Small numbered cores must be above large numbered ones.

2) Small numbered cores have more upper lithology, while large numbered cores have more lower lithology.

3) Horizontal bedding and positively graded bedding can be used as reference marks of a horizontal plane. The angle between core boundary and horizontal line should be approximately equal to the complementary angle of drilling inclination, which is 14.4˚.

4) Many syn-sedimentary deformations can be used to judge core top and bottom, for instance, flame structure, load cast, flute cast, groove cast, intrusive sandstone, liquefied vein *et al.*

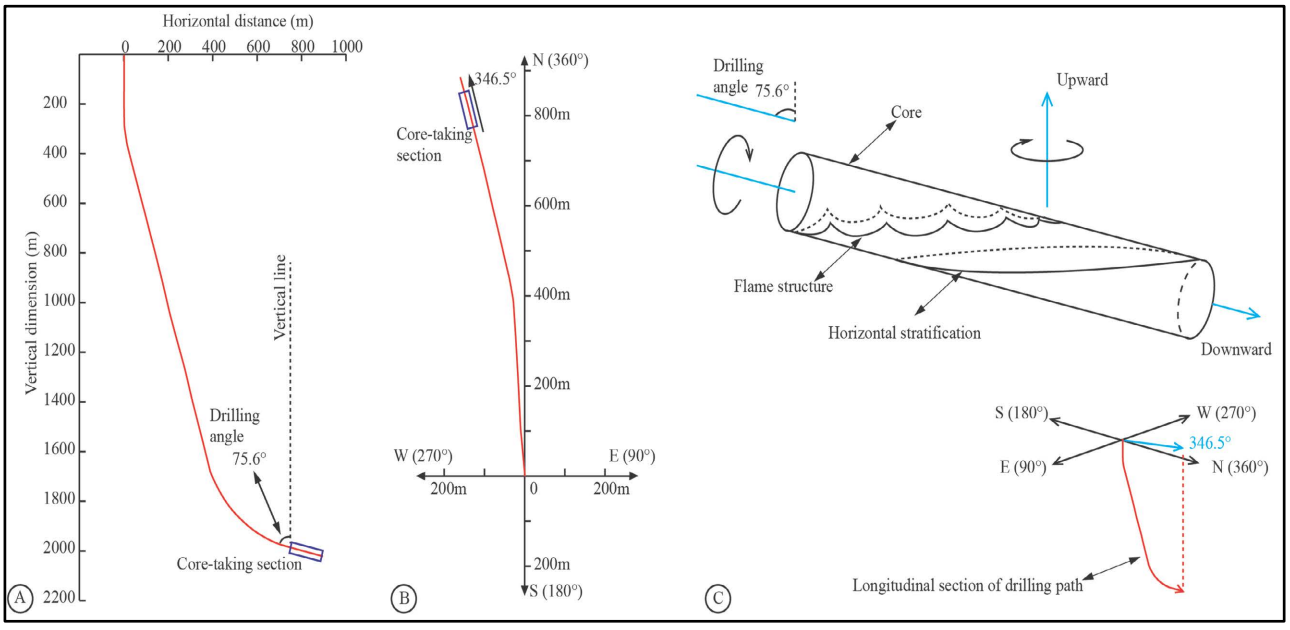

Figure 2. Drilling trajectory and coring section of Well Y in Block X of Huaqing Oilfield, Ordos Basin. (A) Section projection of drilling trajectory. (B) Plane projection of drilling trajectory. (C) The shape and orientation reference of the core section.

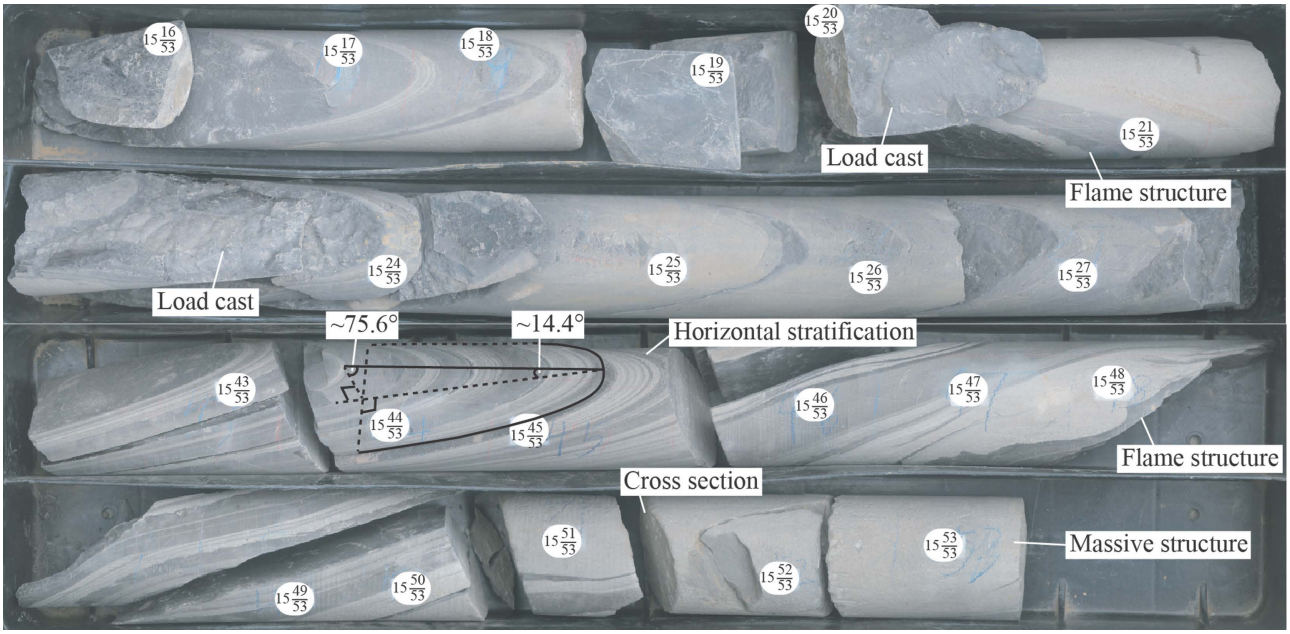

Figure 3. Some typical high-inclination core of well Y in Block X of Huaqing Oilfield, Ordos Basin.

5) Several simulated experiments suggest that the high-density turbidity flow consists of lower sandy debris flow and upper low-density turbidity flow [42] [43] [44]. Alternate conversion between sandy debris flow and turbidity flow frequently occurs during transportation [45] [46]. Turbidity flow deposits with rich top-bottom structures often appear on or near the hard-oriented massive sandstone. They can help orient massive sandstones after the cores are spliced according to the degree of section matching. The orientation of massive sandstone is of great significance. Massive sandstone is the most critical oil reservoir, and the direction of fractures inside massive sandstone affects the deployment of the flooding well network.

Combined with two relatively accurate engineering data, the drilling direction angle and inclination angle, the core can be reset after determining the top and bottom of the core, which is the premise to determine the fracture occurrence and the ancient flow direction of sandy debris flows. Flute cast and partial load cast were used to reconstruct ancient flow directions. For groove cast, nearly symmetrical load cast, and incomplete load cast, ancient flow directions were reconstructed by particle arrangement in bedding structure.

4. Results

4.1. Lithological Characteristics

The first set of results mainly shows the evidence related to the sedimentary environment. As shown in **Figure 4**, sandy debris flows are, on the whole, mainly composed of massive sandstone and thinly interbedded sandstone mudstone. Some of the massive sandstones are also intercalated with thin-bedded muddy siltstone. A significant complete set of horizontal bedding mudstone was deposited during the intermittent deposition of sandy debris flows. There are more

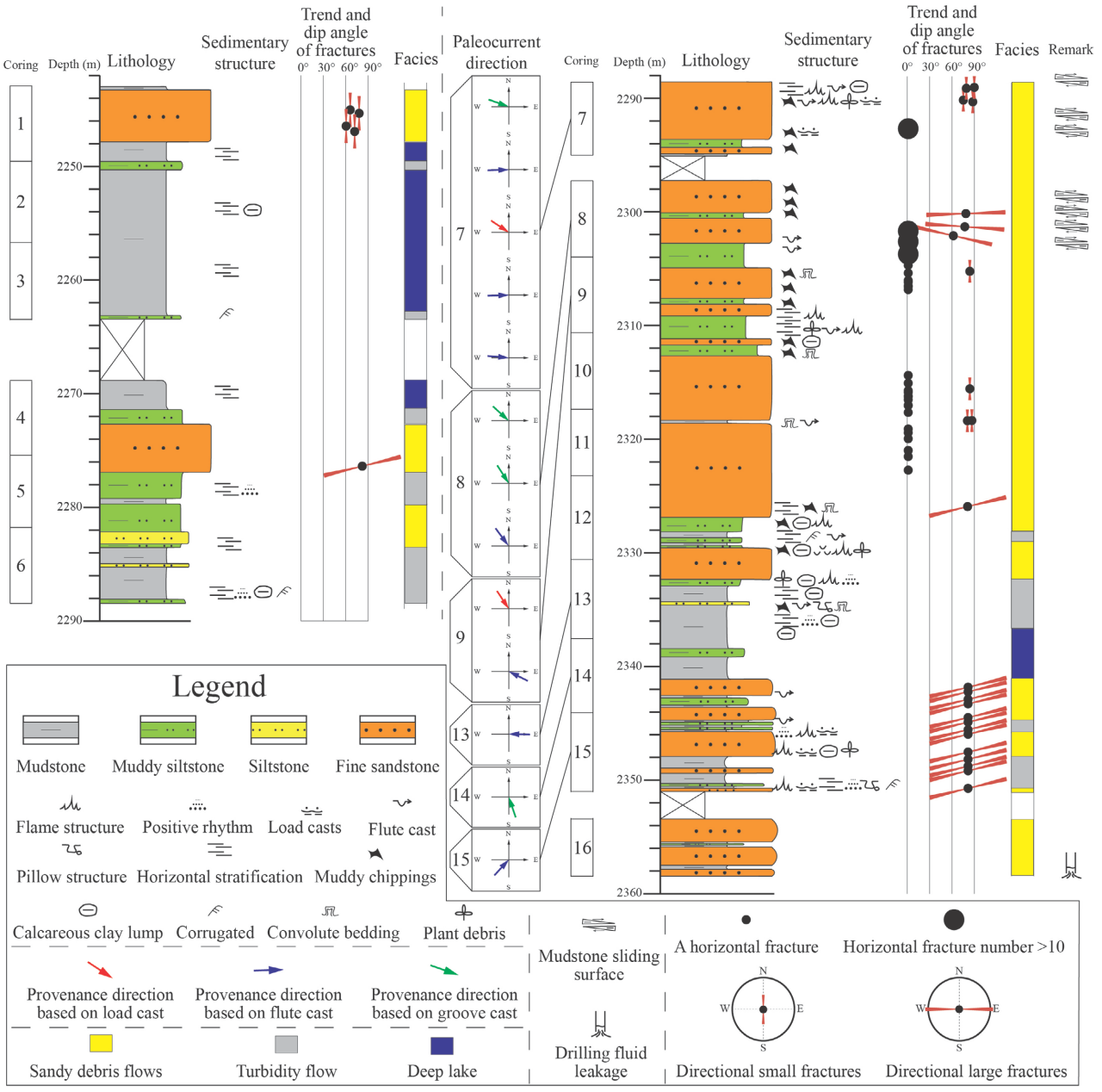

Figure 4. Lithology histogram, sedimentary structure, fracture occurrence statistics, and paleocurrent reconstruction of Y well coring section in block X of Huaqing Oilfield, Ordos Basin.

and richer bedding structures and bedding planes in thinly interbedded sandstone-mudstone than in the large complete set of mudstone and massive sandstone. From bottom to top, the core can be divided into four parts, and a more detailed core description of each part from down to up is shown as follows:

The first part of the core from 2359 to 2341 meters, the characteristic of which is middle-thin layer fine sandstone, thin layer mudstone, and thin layer muddy siltstone interbedded strata. Sandstone mainly comes from sandy debris flow and turbidity flow. The mudstone is characterized by horizontal stratification. The overlying sandstone load on the mudstone causes the deformation of the

mudstone, even sandstone below. Many flame structures and load casts exist between mudstone and fine sandstone (Figure 3). Pillow structures and intrusive sandstone formed when partial sandstones penetrated the mudstone (Figure 5(A)). Positive rhythm is composed of fine sandstone, argillaceous siltstone, and mudstone, and wavy beddings mainly exist in argillaceous siltstone. There is also a small-scale flute cast in thin-laminated mudstone interlayer in middle layer fine sandstone.

The second part of the core is from 2341 to 2327 meters. The characteristic is that an extensive suite of thin mudstone with horizontal stratification contains thin argillaceous siltstone, siltstone, and a small amount of middle-thin layer fine sandstone. Mudstone is a deep lake mudstone, while sandstone comes from turbidite deposition. The upper mudstone in this section contains more lime mudstone lumps, which were encased in black mudstone crust than the lower one (Figure 5(B)). The thin argillaceous siltstone and siltstone contain many lacerated muddy chippings and floating gravels. Water escape structure, ball-and-pillow structure, and flame structure formed by differential compaction

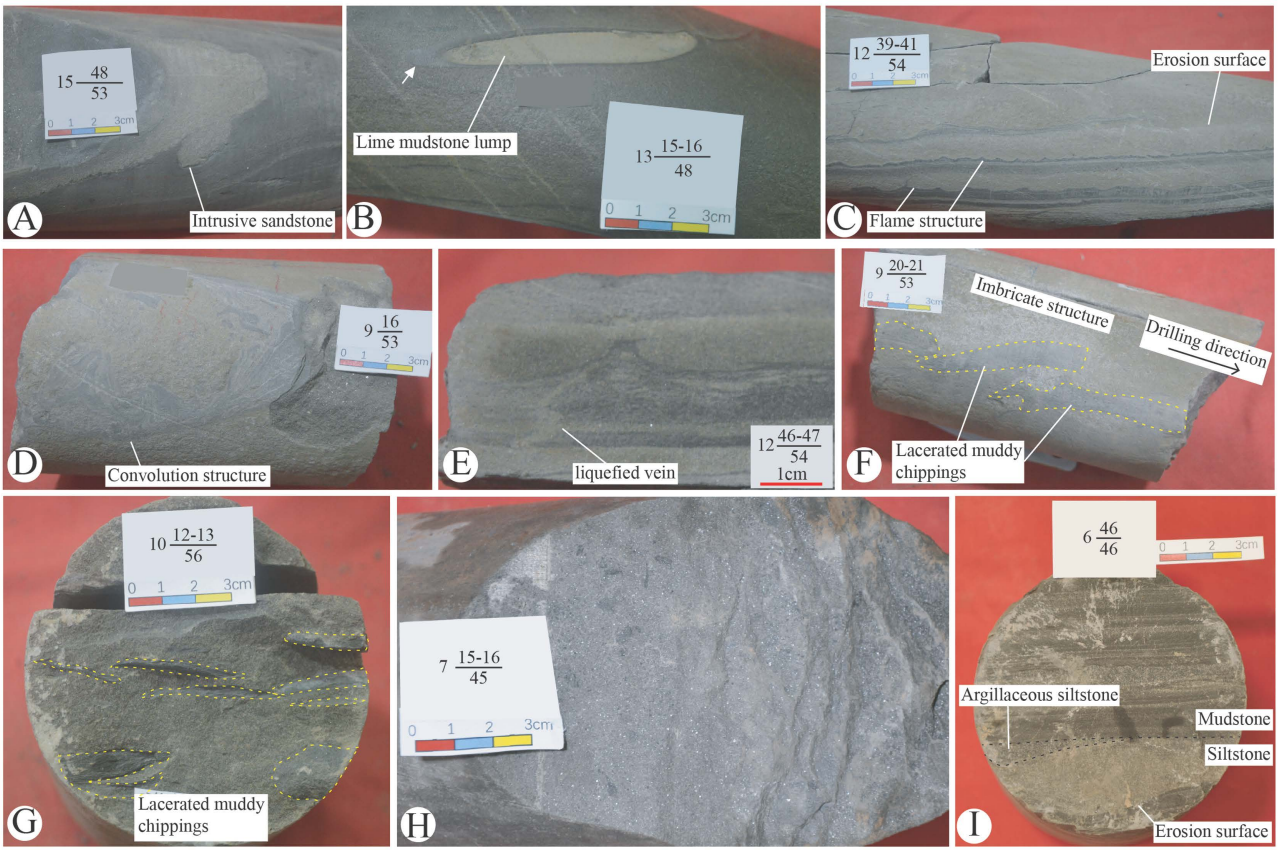

Figure 5. Bedding structures of Well Y core in Block X of Huaqing Oilfield, Ordos Basin. (A) Intrusive sandstone. 15-48/53. (B) Lime mudstone lumps with black argillaceous coating. 13-(15-16)/48. (C) Flame structure and erosion surface. 12-(39-41)/54. (D) Convolution structure. 9-16/53. (E) Liquefied vein. 12-(46-47)/54. (F) Imbricate structure composed of lacerated muddy chippings. 9-(20-21)/53. (G) Characteristics of lacerated muddy chippings in the core section. 10-(12-13)/56. (H) Many small mica fragments in sandstone. 7-(15-16)/45. (I) The gradual transition of fine sandstone with scouring surface to interbedded mudstone and argillaceous siltstone with horizontal bedding. 6-46/46.

can be identified at the lithologic interface of sandstone and mudstone (**Figure 5(C)**). Small-scale flute casts, wavy bedding, and convoluted structure also occur in thin interbedded sandstone and mudstone (**Figure 5(D)** and **Figure 5(E)**).

The third part of the core is from 2327 to 2289 meters. This core section comprises massive fine sandstone and includes interbedded medium-bedded fine sandstone and medium-thin argillaceous siltstone. Sandstones almost all come from sandy debris flow. The upper sandstone erodes most of the argillaceous sediments to form lacerated muddy chippings, which were compressed and deformed and floated in massive sandstone (**Figure 5(F)** and **Figure 5(G)**). Only a few argillaceous sediments are preserved intact to form interlayers. Many large flute casts and flame structures appear in this section. Convoluted structures and loaded structures also occur at the interface between sandstone and mudstone. There are many fine mica fragments in sandstone (**Figure 5(H)**).

The fourth part of the core is from 2289 to 2243 meters. This core section is almost all composed of thin mudstone with horizontal stratification, mainly the deposition of the deep lake environment. Thin argillaceous siltstone and medium-thin sandstone can be observed occasionally. Silty sandstone eroded argillaceous deposits and formed a small scouring surface at the bottom of the core (**Figure 5(I)**).

4.2. Bedding Planes Structures and Ancient Flow Directions

In order to assess ancient flow directions, bedding plane structures with directionality were used (**Figure 6**, **Table 1**). **Figure 4** presents the ancient flow directions of different core sections based on different bedding plane structures. The most exciting aspect of this figure is that the law of ancient flow directions changing with the sedimentary process is shown. When the sandstone of the first core (2359 - 2341 m) was deposited, the sandy debris flow came from the directions of the west by south 43˚ (**Figure 6(A)**) and south by east 19˚ (**Figure 6(B)**). In the deposition process of the second core (2341 - 2327 m), mainly composed of mudstone, the direction of a small amount of sandy debris flow is almost positive east (**Figure 6(C)**).

The core of the third section (2327 - 2289 m) can be further divided into three parts from bottom to top: the lower massive sandstone section (2327 - 2313 m), the middle sand-mud interbed section (2313 - 2303 m), and the upper thick sandstone section (2303 - 2289 m). The lower massive sandstone section lacks directional bedding plane structures. In contrast, the other two sections have preserved more bedding structures because of their middle layer mudstone and medium-thick layer sandstone. When the sandstone of the middle sand-mud interbed section was deposited, the sandy debrite came from the south by east 64˚ (**Figure 6(D)**) and north by west 34˚ (**Figure 6(E)**). Among them, the sandy debris flows from the north by west 34˚ has a pronounced load cast due to its considerable thickness. The direction of sandy debris flow in the eighth coring is almost the same as that in the ninth. The directions of sandy debris flow in the

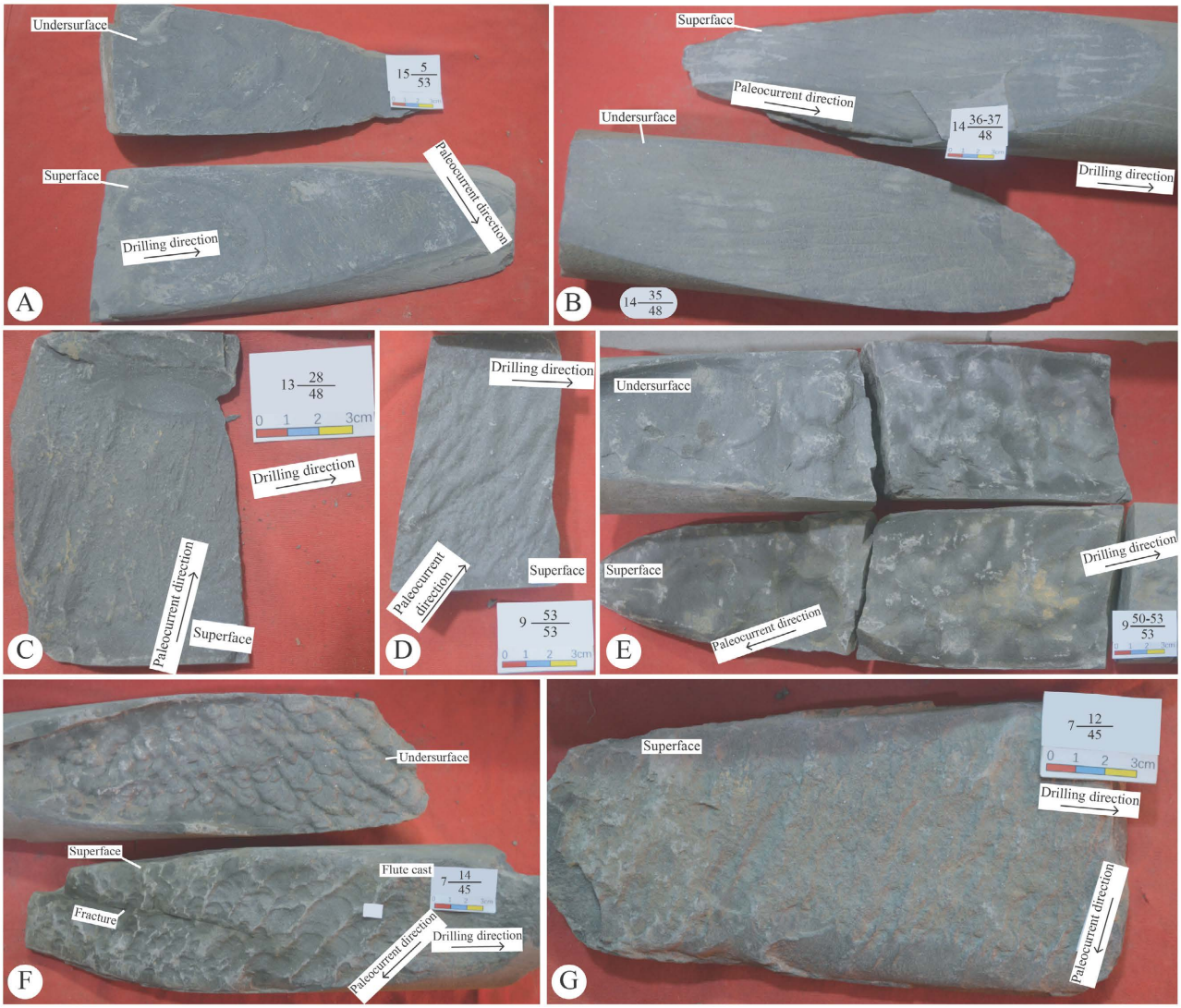

Figure 6. Bedding plane structures of Well Y core in Block X of Huaqing Oilfield, Ordos Basin. (A) Small-scale flute cast. 15-5/53. (B) Groove cast. 14-(36-37)/48. (C) Small-scale flute cast. 13-28/48. Superface. (D) Small-scale flute cast. 9-53/53, Superface. (E) Load cast. 9-(50-53)/53. (F) Large-scale flute cast. 7-14/45. (G) Small-scale flute cast. 7-12/45. Superface.

seventh coring are favorable west and west by north 33˚. The evident and large flute casts were formed under the erosion of sandy debris flow in the west direction by north 33˚ (**Figure 6(F)**), while the fuzzy and small flute casts were formed after the flow-through of sandy debris in the west direction (**Figure 6(G)**). The ancient flow direction of sandy debris flow is highly consistent with the sandstone thickness map, drawn under the limitation of more than hundreds of wells in November 2021 (**Figure 7(A)**). Based on a small-scale flute cast, the reconstructed paleocurrent direction has a current from the East, and the latest drilling results based on June 2022 show that there is indeed a sandy belt to the east of the well (**Figure 7(B)**). The drilling results in 2022 show that the high-inclination drilling in the Northwest and North has the highest drilling ratio of sandstone in the high angle section (**Figure 7(B)**, **Figure 8**). These two directions

Table 1. Ancient flow direction of sandy debris flows reconstructed from different bedding plane structures of well Y core in block X of Huaqing Oilfield, Ordos Basin.

Number of coring	Number of sample	Paleocurrent direction of sandy debris flow	Bedding plane structures
7	3	289˚	Groove cast
7	12	268˚	Small-scale flute cast
7	13 - 14	303˚	Load cast
7	14	268˚	Large-scale flute cast
7	8 - 11	275˚	Small-scaleflute cast
8	11 - 14	312˚	Groove cast
8	40 - 42	327˚	Groove cast
8	48 - 50	323˚	Small-scale flute cast
9	50 - 53	326˚	Load cast
9	53	116˚	Small-scale flute cast
13	28	90˚	Small-scale flute cast
14	35 - 37	161˚	Groove cast
15	5	223˚	Groove cast

*The north is considered 0˚, and the east is considered 90˚.

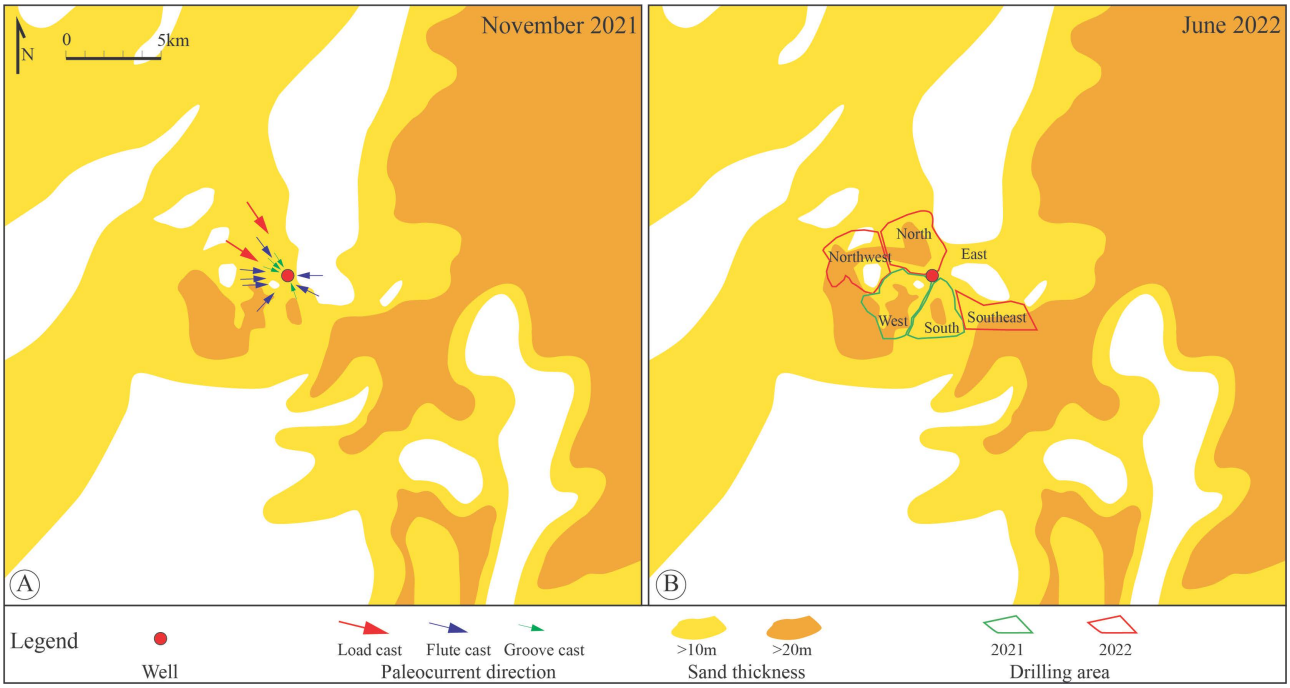

Figure 7. Sand thickness and ancient flow direction of well Y core in block X of Huaqing Oilfield, Ordos Basin.

are also consistent with the direction of paleocurrent restored by load casts and large-scale flute casts (**Figure 7(A)**).

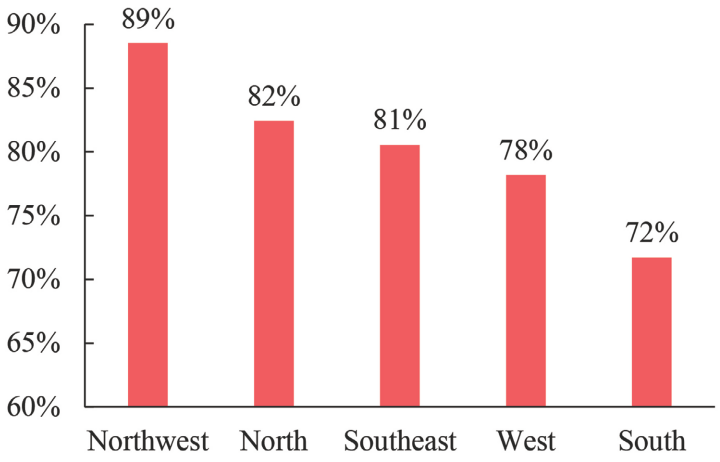

Figure 8. The drilling rate of sandstone in the high-inclination section around well Y core in block X of Huaqing Oilfield in 2022.

4.3. Fracture Occurrence

Since fracture trends are of great significance to low permeability sandstone reservoirs development, the trend of natural fractures of the core sandstone section is described in this paper. The sandstone section is roughly divided into three parts: the bottom sand-mudstone interbed section (2359 - 2341 m), the middle massive sandstone section (2327 - 2289 m), and the upper middle-layered sandstone section (2283 - 2271 m and 2248 - 2243 m).

From **Figure 4**, it can be seen that there are apparent differences between fracture types and fracture density of the core sandstone section. The bottom sand-mudstone interbed section (2359 - 2341 m) is dominated by high-angle NEE-SWW-trending fractures, and the dip angle is about 65˚ - 80˚ (**Figure 9(A)**). These fractures have large openings and are filled with calcite and other fillings (**Figure 9(B)**). It is worth noting that the core loss occurred when drilling at this section, resulting in the 16th coring incomplete.

The unfilled near-horizontal low angle and horizontal fractures mainly develop the middle massive sandstone section (2327 - 2289 m), accompanied by some N-S-trending unfilled fractures (**Figure 6(F)**; **Figure 9(C)** and **Figure 9(D)**). The density of low angle and horizontal fractures increases gradually from bottom to top (**Figure 9(E)**). Sliding surfaces often occur in the most developed areas of horizontal fractures (**Figure 9(F)**). The sliding surface of mudstone has a scratch of the north by west 18˚ and a fault step of the east by north 41˚ (**Figure 9(G)**). The middle massive sandstone section also has a small number of fractures with high angle NEE-SWW-trending fractures and minor unfilled fractures in the north direction.

There are few fractures in the upper middle-layered sandstone section (2283 - 2271 m and 2248 - 2243 m), mainly half-filled fractures in the north direction, and the fracture angle is about 60˚ (**Figure 9(H)**). There are also some unfilled fractures at the lithologic interface in this section (**Figure 9(I)**).

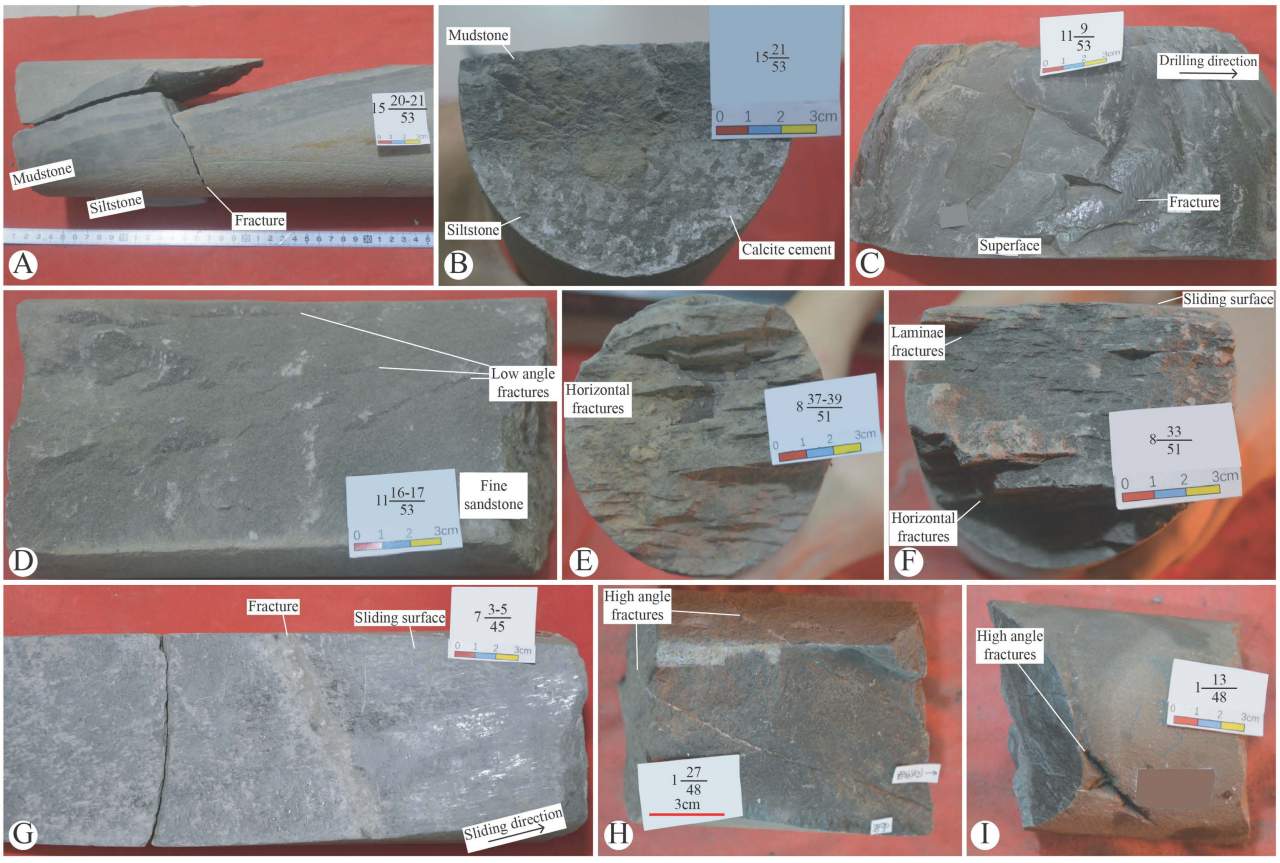

Figure 9. Fracture occurrence of Well Y core in Block X of Huaqing Oilfield, Ordos Basin. (A) High angle NEE-SWW-trending fractures. 15-(20-21)/53. (B) Calcite cement on the high angle fracture surface. 15-21/53. (C) Unfilled high-angle small N-S-trending fractures. 11-9/53. (D) Low angle fractures in massive fine sandstone. 11-(16-17)/53. (E) Horizontal fractures in fine sandstone. 8-(37-39)/51. (F) Horizontal fractures in fine sandstone and laminae fractures in mudstone. 8-33/51. (G) Sliding surface. 7-(3-5)/45. (H) High angle fractures filled with calcite. 1-27/48. (I) Unfilled high-angle S-N-trending fractures. 1-13/48.

5. Discussion

5.1. Ancient Flow Direction of Sandy Debris Flows

As mentioned in the in the earlier part of this paper, the ancient flow direction reconstruction results are more instructive than the provenance direction for predicting deep-water sandy debris flow reservoirs. The thick sandstone of the Chang-6 gravity-flow deposit resulted from tectonic activity in the Qinling area [18]. The sandy debris flow in the study area is a channel-type gravity flow with the erosive ability and is similar to the riverside deposit (**Figure 5(I)**) [46]. Many load casts, flute casts, and groove casts were formed in the sedimentary stage of sandy debris flow, providing a solid foundation for reconstructing the ancient flow direction (**Figure 6**).

According to these data, we can infer that the ancient flow direction of sandy debris flows gradually shifts from southwest and southeast to northwest and west from bottom to top of the core (**Figure 4**). The first part of the core (2359 - 2341 m) is the interbedded sandstone-mudstone deposition formed by the sandy debris flow from southwest and southeast and the turbidity flow deposition se-

parated from the sandy debris flow. The sandstone may be the direct product of the Middle Indosinian tectonic activity in the Qinling orogenic belt. The second part of the core (2341 - 2327 m) includes deep lake mudstone, sandy debris flow, and turbidity flow. Notably, sandy debris flows come from the east and contain large amounts of lime mudstone lumps with black argillaceous coating, formed in shallow lake environment and migrated to the deep lake with the sliding of sandy debris flow [47]. One possible explanation is that the northeast delta slumped from the east into the Huaqing area. The sandstone provided minor from southwest provenance. The third part of the core (2327 - 2289 m) mainly comprises sandy debris flow from the northwest, most likely coming from the northeast Wuqi delta, and slipped from the north into the Huaqing Oilfield [48]. The sandy debris flow entered the Huaqing area from the northwest by the lake bottom topography. The western provenance is likely to be the collapse of the braided river delta in the southwest caused by the strengthening of the Qinling activity. The sandy debris flow entered the Huaqing oilfield from the west. The existence of many mica fragments in the core suggests that the braided river delta in the west may be the primary provenance (**Figure 5(H)**). The crushing of mudstone interlayer formed lacerated muddy chippings during the transport of sandy debris flow (**Figure 5(B)** and **Figure 5(G)**) [49]. Many lacerated muddy chippings exist in the upper part of sandy debris flow.

The research result of ancient flow direction is reliable because it is highly consistent with the sandstone thickness. Among all the ancient flow directions, sandy debris flow mainly enters the study area from north to west, and turbidity flow primarily comes from the west. Because southwest provenance has a shorter migration distance and is conducive to the preservation of mica, many mica in sandstone also indicates that the slump sandstone may come from braided river delta front in the southwest of the Huaqing area. So the southwest direction may be a secondary provenance supply direction (**Figure 5(H)**). The current study's findings do not support the previous research results that ancient flow directions of sandy debris flow were the northeast in Huaqing Oilfield [11]. At least the sandy debris flow did not enter the study area directly from the northeast. This finding was unexpected and suggested that the ancient flow directions of sandy debris flow should be from the northwest because the northwest is never the focus of researchers. However, this inconsistency may be due to the topography beneath the lake.

Load cast and large-scale flute casts had more extensive scale and more obvious mudstone deformation and may be related to more significant sandy debris flow, while the small-scale flute casts and groove casts are more related to the turbidity current associated with the sandy debris flows, and are also substantial evidence for the ancient flow direction judgment. The shallow groove cast and small fuzzy flute casts must combine with the bedding structure to reconstruct ancient flow directions. Sandy debris flows are mostly confined flow, while turbidity flows are more likely to be offset by isobath flow and become

unconfined flow [50]. Thus, the directional load cast and large-scale flute casts were considered more reliable evidence in the comprehensive summary of the ancient flow direction. The ancient flow directions reconstructed from flute casts were more precise than those from load casts. Thus, it is essential to consider the possible bias in our conclusions on the ancient flow directions (**Figure 6**).

5.2. Fracture Genesis

An initial objective of the core orientation was to identify the direction of tiny natural fractures. Prior studies have noted the importance of natural fractures in tight reservoirs development in the Ordos Basin. Several reports have shown that the fracture direction is mainly NWW spreading in Chang-6 Member. The fracture might result from different stress fields in Yanshanian and Himalayan periods or local plastic deformation of shale [21] [23] [28]. The western margin of the Ordos Basin experienced N-S compression in Indosinian, NW-SE compression in Yanshanian, and NNE-SSW compression in Himalayan [51]. The fracture orientations include NE-SW, NNE-SSW, NW-SE, and NNW-SSE. Some NE-SW-trending fractures were developed in the N-S compression environment in the Indosinian period [52]. The NW-SE-trending fractures formed in the Yanshanian period, while the N-S-trending fractures formed in the Himalayan period [31].

After repeatedly comparing our fracture orientation results with previous research results, the results of fracture orientation are shown in **Figure 10**. A small amount of NE-SW-trending fractures formed in Indosinian, and mudstone sliding surface and NEE-SWW-trending fractures were formed in Yanshanian [25].

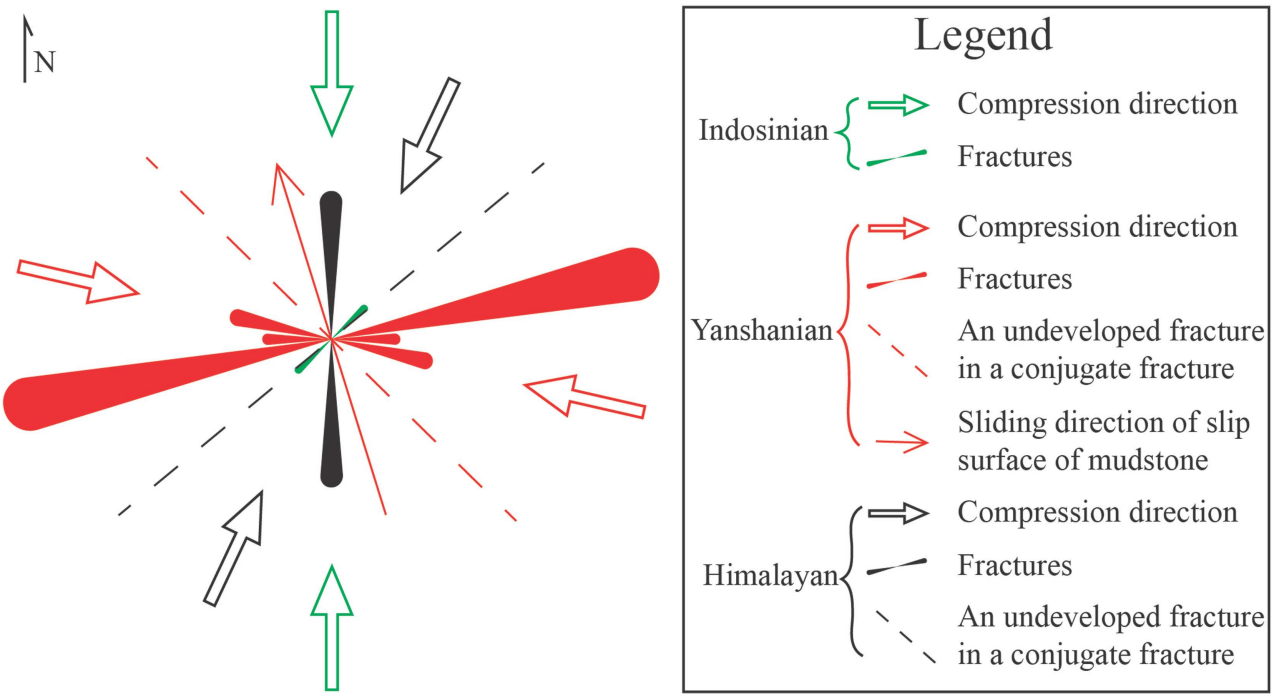

Figure 10. The extrusion direction and fracture direction in different structural periods of Huaqing Oilfield, Ordos Basin.

The high angle NEE-SWW-trending fractures at the bottom of the coring section have the most significant influence on the seepage capacity of the reservoir because they not only disconnect the core but also cause the leakage of drilling fluid (**Figure 5(B)**). This finding is consistent with Fan *et al.* (2016), who suggest that the NE-SW-trending fractures dominate seepage flow direction.

The density of horizontal fractures gradually increases during the transformation from massive sandstone to sand-shale interbed, and mudstone slippage occurs where the most significant fracture density of horizontal fractures (**Figure 9(G)**). The horizontal fractures developed in the central massive sandstone section are more like shear fractures under shear stress than diagenetic fractures. This explanation contradicts previous studies, which have suggested that the horizontal fractures developed in the central massive sandstone section are diagenetic [53]. In the flow process of sandy debris flow, there was shear stress in any internal layer, so near-horizontal low angle fractures were formed in the massive sandstone (**Figure 9(D)**) [49]. The low angle and horizontal fractures are more developed in mudstone because of the different shear strength between sandstone and mudstone (**Figure 9(F)**). Under the NW-SE compression in Yanshanian, the strike of the large fracture is not consistent with the NEE-SWW-trending fracture in the core section where the mudstone slip surface develops. A possible explanation for this might be that the detachment of rock strata along the mudstone surface and the deformation of rock strata offset the component of NW-trending compressive stress along the NW direction.

The E-W component of NW-SE compressive stress along high-angle cracks forms E-W-trending fractures, even SEE-NWW-trending cracks. This explanation agrees with Zhao's [24] findings, showing that fracture strike in vertical strata is also affected by mudstone slippage. The formation period of the E-W-trending fracture is also consistent with those of Tian [30], who declared that E-W-trending fractures of the Yanchang Formation were mainly formed at terminal Jurassic-Early Cretaceous, that is, the Yanshanian period. During the Himalayan period, the NNE-SSW compression formed nearly N-S-trending fractures, similar to Jiyuan Oilfield in northwestern Huaqing Oilfield [54].

Notably, these high-inclination coring may be somewhat limited in fracture orientation when the formation is inclined, the core is broken, and the poorly matched core section. In addition, the research results of fractures are based on the relationship between fracture direction and cutting and combined with previous understanding. Thus, there are some deficiencies in the research conclusions of fracture stages due to the lack of data on cement inclusions and cement dating. Therefore, a further study focusing on the combination of fracture orientation of high-inclination core and cement aging is suggested.

5.3. Significance of High-Inclination Coring

High-inclination coring has many advantages and excellent utilization space. The present results are significant in at least two critical respects of paleocurrent re-

construction and fracture orientation. The present study suggests that vertical coring is used to determine the coring horizon, and the high-inclination coring is used to reconstruct the ancient flow direction. The combination of the two guides the exploration and rolling development of deep-water sandy debris flow tight reservoirs to significantly reduce the number of exploration wells. The ancient flow direction predicted by this high-inclination coring is successful because it is consistent with the law of sandstone distribution determined by hundreds of exploration wells. Even there is a possibility to provide more accurate distribution direction for different layers of sandstone.

It is worth noting that there are few bedding structures and single bedding structures in massive sandstone and mudstone of deep lacustrine sandy debris flow. Before high-inclination coring, the coring section should refer to the vertical coring of nearby exploration wells or evaluation wells. The coring section should be screened according to different research purposes. The sand-mud interbedded area is the best core location because it might retain information about ancient flow direction. The massive sandstone area is the best core location for reservoir fracture study because it is the main oil-bearing area in most cases.

There is no noticeable increase in technical difficulty and coring cost for high-inclination wells relative to vertical coring. However, it provides an excellent data foundation for the scrolling development and the deployment of the flooding well network. In addition, high-inclination coring can provide 3 - 4 times the long core data of vertical coring at the same depth and take the change of horizontal permeability in the vertical direction. It is of great significance for the oil-water flooding experiments of ultra-low permeability reservoirs. Although high-inclination coring cannot wholly replace vertical coring of exploration wells and evaluation wells, combining high-angle coring and vertical coring can significantly reduce the number of exploration wells and evaluation wells. There is also enormous room for further progress with this method in the exploration and scrolling development of tight sandstone reservoirs.

The slight dip angle of the Yanchang Formation in Ordos Basin makes the horizontal bedding not deviate too much from the horizontal plane; the tight lithology makes the core not easy to rupture, which is conducive to rock splicing. Therefore, the Yanchang Formation is very suitable for high slope coring orientation. The reconstruction of ancient flow direction is relatively accurate, and fracture orientation also has a relatively small error. High-inclination coring is worthy of promotion in areas where tight deep-water reservoirs are developed with slight dip angles and weak tectonic activity.

6. Conclusions

1) High-inclination coring is an essential means for core orientation. Relatively accurate microfracture direction and ancient flow direction can be obtained after core orientation, which has guiding significance for the exploration and scrolling

development of deep-water tight sandstone reservoirs.

2) The ancient flow direction of sandy debris flow in the Huaqing area gradually shifts from southwest and southeast to northwest and west from bottom to the top of the core. Massive sandstone of sandy debris flow, which probably comes from the Wuqi Delta, mainly enters the study area from the northwest. Turbidity flow likely to come from Southwest provenance primarily slipped into the Huaqing region from the west.

3) A small amount of NE-SW-trending fractures were formed in the Indosinian period. The horizontal and low-angle fractures in massive sandstone are shear fractures formed in sand debris flow collapse. Mudstone sliding surface and NEE-SWW-trending fractures were formed in the Yanshanian period. During the Himalayan period, the compression from the southwest resulted in a development fracture of conjugate fracture, forming nearly N-S-trending fractures.

Fund

This study was financially supported by the Key Technology of Effective Productivity Construction and Guiding Field Test of Tight Oil in Changqing Oilfield (Grant Nos. 2022KT1104).

Acknowledgements

The authors would like to thank Yong Zhang and Shengwei Miao of Zhongshuo Company for the convenience they provided in the process of core observation. The author would like to congratulate Lumin Shi and Baishun Shi for their guidance and assistance in core observation.

Conflicts of Interest

The authors declare no conflicts of interest regarding the publication of this paper.

References

[1] Yang, H., Fu, J., He, H., Liu, X., Zhang, Z. and Deng, X. (2012) Formation and Distribution of Large Low-Permeability Lithologic Oil Regions in Huaqing, Ordos Basin. *Petroleum Exploration and Development*, **39**, 683-691. https://doi.org/10.1016/S1876-3804(12)60093-7

[2] Fu, S., Deng, X. and Pang, J. (2010) Characteristics and Mechanism of Thick Sandbody of Yanchang Formation at the Centre of Ordos Basin. *Acta Sedimentologica Sinica*, **28**, 1081-1089.

[3] Li, X., Fu, J., Guo, Y., Wanyan, R., Chen, Q., Liu, X., Liao, J., Wei, L., Liu, H. and Huang, J. (2011) The Concept of Sandy Debris Flow and Its Application in the Yanchang Formation Deep Water Sedimentation of the Ordos Basin. *Advances in Earth Science*, **26**, 286-294.

[4] Pang, X., Chen, C., Zhu, M., He, M., Liu, B., Shen, J. and Lian, S. (2007) Frontier of the Deep-Water Deposition Study. *Geological Review*, **53**, 36-43.

[5] Yu, X. and Li, S. (2009) The Development and Hotspot Problems of Clastic Petro-

leum Reservoir Sedimentology. *Acta Sedimentologica Sinica*, **27**, 880-895.

[6] Fu, J., Deng, X., Zhang, X., Luo, A. and Nan, J. (2013) Relationship between Deep-water Sandstone and Tight Oil of the Triassic Yanchang Formation in Ordos Basin. *Journal of Palaeogeography*, **15**, 624-634.

[7] Yang, H., Li, S. and Liu, X. (2013) Characteristics and Resource Prospects of Tight Oil and Shale Oil in Ordos Basin. *Acta Petrolei Sinica*, **34**, 1-11.

[8] Wang, X., Ren, L., He, Y., Xi, T., Ge, Y., Mi, N. and Deng, N. (2016) Definition of Tight Oil in Ordos Basin. *Petroleum Geology and Recovery Efficiency*, **23**, 1-7.

[9] Ran, Y. and Zhou, X. (2020) Sedimentary Characteristics and Petroleum Geological Significance of the Chang6 Gravity Flow in the Southwest Ordos Basin. *Acta Sedimentologica Sinica*, **38**, 571-579.

[10] Yao, J., Deng, X., Zhao, Y., Han, T., Chu, M. and Pang, J. (2013) Characteristics of Tight Oil in Triassic Yanchang Formation, Ordos Basin. *Petroleum Exploration and Development*, **40**, 150-158. https://doi.org/10.1016/S1876-3804(13)60019-1

[11] Long, L., Liao, J., Li, Z. and Wang, H. (2012) Characteristics and Genesis of Thick Sandbody in the Centre of Lake Basin in Ordos Basin by Taking the 6th Member of Yanchang Formation in Huaqing Area for Example. *Journal of Oil and Gas Technology*, **34**, 23-27, 32.

[12] Liu, F., Zhu, X., Liang, J., Chen, G. and Liu, T. (2020) Lithofacies Characteristics of Gravity Flow Deposits and Their Impacts on Reservoir Quality in the Yanchang Formation, Ordos Basin. *Marine Geology Frontiers*, **36**, 46-55.

[13] Xian, B., An, S. and Shi, W. (2014) Subaqueous Debris Flow: Hotspots and Advances of Deep-Water Sedimention. *Geological Review*, **60**, 39-51.

[14] Luo, J., Li, Z., Shi, C., Li, J., Han, Y., Wang, H., Li, J. and Wang, C. (2008) Depositional Systems and Provenance Directions for the Chang 6 and Chang 8 Reservoir Groups of the Upper Triassic Yanchang Formation in the Southwestern Ordos Basin, China. *Geological Bulletin of China*, **152**, 101-111.

[15] Li, J., Li, P. and Xu, L. (2009) Provenance Analysis of Chang6Period in Huaqing Area of Ordos Basin. *Journal of Yangtze University*, **6**, 48-51+347.

[16] Li, P., Xu, L. and Li, J. (2010) Provenances of the Chang 6 Oil Measures in the Huaqing Region, Ordos Basin. *Sedimentary Geology and Tethyan Geology*, **30**, 61-65.

[17] Liao, J., Li, Z., Long, L., Yang, J. and Yang, J. (2013) The Effect of Provenance Intersection on the Petroleum Enrichment—An Example from Chang-6 Member in Huaqing Area of Central Ordos Basin. *Xinjiang Petroleum Geology*, **34**, 20-23.

[18] Yang, H. and Deng, X. (2013) Deposition of Yanchang Formation Deep-Water Sandstone under the Controi of Tectonic Events, Ordos Basin. *Petroleum Exploration and Development*, **40**, 513-520. https://doi.org/10.1016/S1876-3804(13)60072-5

[19] Liao, J., Zhu, X., Deng, X., Sun, B. and Hui, X. (2013) Sedimentary Characteristics and Model of Gravity Flow in Triassic Yanchang Formation of Longdong Area in Ordos Basin. *Earth Science Frontiers*, **20**, 29-39.

[20] Li, W., Liu, X., Zhang, Q., Guo, Y., Li, K., Yuan, Z., Wang, Y., Ma, Y., Bai, J., Yang, B. and Li, Z. (2019) Deposition Evolution of Middle-Late Triassic Yanchang Formation in Ordos Basin. *Journal of Northwest University* (*Natural Science Edition*), **49**, 605-621.

[21] Zhang, Y., Zhao, X. and Jiao, J. (2018) Characteristics and Major Control Factors of Natural Fractures in Chang 6 Formation in Ansai Area, Ordos Basin. *Complex Hydrocarbon Reservoirs*, **11**, 25-30.

[22] Fan, J., Qu, X., Wang, C., Lei, Q., Cheng, L. and Yang, Z. (2016) Natural Fracture Distribution and a New Method Predicting Effective Fractures in Tight Oil Reservoirs in Ordos Basin, NW China. *Petroleum Exploration and Development*, **43**, 806-814. https://doi.org/10.1016/S1876-3804(16)30096-9

[23] Wang, Q., Zheng, R., Liang, X., Xin, H. and Wang, C. (2011) Feature and Genesis of the Reservoir Fractures of Upper Triassic Yanchang Formation in Jiyuan Area, Ordos Basin. *Journal of Chengdu University of Technology* (*Science & Technology Edition*), **38**, 220-228.

[24] Zhao, X., Zeng, L., Wang, X., Wang, F., Zhang, Y., Jiao, J. and Weng, J. (2015) Differences of Natural Fracture Characteristics and Their Development Significance in Chang 6, Chang 7 and Chang 8 Reservoir, Ningxian-Heshui Area, Ordos Basin. *Chinese Journal of Geology*, **50**, 274-285.

[25] Zeng, L., Li, Z., Shi, C., Wang, Z., Zhao, J. and Wang, Y. (2007) Characteristics and Origin of Fractures in the Extra Low-Permeability Sandstone Reservoirs of the Upper Triassic Yanchang Formation in the Ordos Basin. *Acta Geologica Sinica*, **81**, 174-180.

[26] Su, H., Lei, Z., Zhang, D., Li, J., Zhang, Z., Ju, B. and Li, Z. (2017) Dynamic and Static Comprehensive Prediction Method of Natural Fractures in Fractured Oil Reservoirs: A Case Study of Triassic Chang 63 Reservoirs in Huaqing Oilfield, Ordos Basin, NW China. *Petroleum Exploration and Development*, **44**, 972-982. https://doi.org/10.1016/S1876-3804(17)30109-X

[27] Ma, S., Lin, W., Wang, Q., Xu, H., Wang, X., Zhang, L. and Jiang, C. (2016) Shear Fracture Direction and Mechanical Characteristics of the Middle Yanchang Formation, Southern Ordos Basin, China. *Chinese Science Bulletin*, **61**, 3049-3063. https://doi.org/10.1360/N972016-00469

[28] Li, H., Zhang, M., Pu, R., Zhang, J. and Ding, G. (2017) Late Triassic Fracture Detection with Seismic Azimuth Anisotropics in Huang 257 Survey, Ordos Basin. *Oil Geophysical Prospecting*, **52**, 350-359+196.

[29] Zhou, X., Zhang, L., Huang, C. and Wan, X. (2012) Distraction Network Conceptual Model and Validity of Fractures in Chang 6_3 Low Permeable Reservoir in Huaqing Area. *Journal of Jilin University. Earth Science Edition*, **42**, 689-697.

[30] Tian, Y., Shi, Z., Song, J., Wu, X., Gao, X. and Zou, Y. (2009) Characteristics of Fractures in the Sandstone Reservoirs of Yanchang Formation in Southeastern Ordos Basin. *Journal of Geomechanics*, **15**, 281-288.

[31] Xiao, Z., Ding, W., Liu, J., Tian, M., Yin, S., Zhou, X. and Gu, Y. (2019) A Fracture Identification Method for Low-Permeability Sandstone Based on R/S Analysis and the Finite Difference Method: A Case Study from the Chang 6 Reservoir in Huaqing Oilfield, Ordos Basin. *Journal of Petroleum Science and Engineering*, **174**, 1169-1178. https://doi.org/10.1016/j.petrol.2018.12.017

[32] Zou, C., Wang, L., Li, Y., Tao, S. and Hou, L. (2012) Deep-Lacustrine Transformation of Sandy Debrites into Turbidites, Upper Triassic, Central China. *Sedimentary Geology*, **265-266**, 143-155. https://doi.org/10.1016/j.sedgeo.2012.04.004

[33] Liu, F., Zhu, X., Li, Y., Xu, L., Niu, X., Zhu, S., Liang, X., Xue, M. and He, J. (2015) Sedimentary Characteristics and Facies Model of Gravity Flow Deposits of Late Triassic Yanchang Formation in Southwestern Ordos Basin, NW China. *Petroleum Exploration and Development*, **42**, 577-588. https://doi.org/10.1016/S1876-3804(15)30058-6

[34] Xia, Q. and Tian, J. (2007) Sedimentary Characteristics of Sublacustrine Fan of the Interval 6 of Yanchang Formation of Upper Triassic in Southwestern Ordos Basin.

Journal of Palaeogeography, **9**, 33-43.

[35] Zhang, Y., Li, S., Tian, J., Zhou, X. and Yang, T. (2021) Sedimentation Types of Deep-Water Gravity Flow, Chang7 Member, Upper Triassic Yanchang Formation, Ordos Basin. *Acta Sedimentologica Sinica*, **39**, 297-309.

[36] Zhou, Y., Cheng, X., Ma, L., Wei, L., Liu, X., Fan, W., Wang, H. and Wu, H. (2015) The Principles and Methods on Determining Spatial Orientation of Sandstones and Fractures in Subsurface Reservoir. *Progress in Geophysiscs*, **30**, 1243-1250.

[37] Lei, J., Jiang, X. and He, Z. (2018) Paleomagnetic Orientation Analysis of Macroscopic Natural Fractures at Yanchang Formation in Northeast Yanchang Oilfield. *Northwestern Geology*, **51**, 272-276.

[38] Liu, P. (2019) Magnetic Behavior of Rocks and Forward and Inverse Models Incorporating Demagnetization. Doctoral Thesis, China University of Geosciences, Wuhan.

[39] Chen, Z., Fu, L., Chen, X., Zhang, T., Xie, Y., Wang, H. and Zhu, Y. (2021) Quantitative Evaluation Method for Micro Heterogeneity of Tight Sandstone: A Case Study of Chang-6 Reservoir of Yanchang Formation in Huaqing Area, Ordos Basin. *Acta Sedimentologica Sinica*, **39**, 1086-1099.

[40] Deng, X., Luo, A., Zhang, Z. and Liu, X. (2013) Geochronological Comparison on Indosinian Tectonic Events between Qinlin Orogeny and Ordos Basin. *Acta Sedimentologica Sinica*, **31**, 939-953.

[41] Fu, Q., Li, J., Deng, X., Zhao, S., Pang, J. and Meng, P. (2019) Influence of Sedimentary Events on Deep Water Sedimentation Process: A Case of Chang 6 Reservoir in Huaqing Area, Ordos Basin. *Lithologic Reservoirs*, **31**, 20-29.

[42] Postma, G., Nemec, W. and Kleinspehn, K.L. (1988) Large Floating Clasts in Turbidites: A Mechanism for Their Emplacement. *Sedimentary Geology*, **58**, 47-61. https://doi.org/10.1016/0037-0738(88)90005-X

[43] Shanmugam, G. (1996) High-Density Turbidity Currents; Are They Sandy Debris Flows? *Journal of Sedimentary Research*, **66**, 2-10. https://doi.org/10.1306/D426828E-2B26-11D7-8648000102C1865D

[44] Shanmugam, G. (1997) The Bouma Sequence and the Turbidite Mind Set. *Earth-Science Reviews*, **42**, 201-229. https://doi.org/10.1016/S0012-8252(97)81858-2

[45] Shanmugam, G., Shrivastava, S. and Das, B. (2009) Sandy Debrites and Tidalites of Pliocene Reservoir Sands in Upper-Slope Canyon Environments, Offshore Krishna-Godavari Basin (India): Implications. *Journal of Sedimentary Research*, **79**, 736-756. https://doi.org/10.2110/jsr.2009.076

[46] Fu, J., Luo, S., Niu, X., Lv, Q., Xu, L., Feng, S. and Li, S. (2015) Sedimentary Characteristics of Channel Type Gravity Flow of the Member 7of Yanchang Formation in the Longdong Area, Ordos Basin. *Bulletin of Mineralogy, Petrology and Geochemistry*, **34**, 29-37+21.

[47] Liao, J., Li, X., Li, Z., Zhao, H., Wanyan, R., Zhang, X. and Wang, J. (2017) Genetic Mechanism of Mud-Coated Intraclasts within Deep-Water Massive Sandstone in Yanchang Formation, Ordos Basin. *Journal of China University of Petroleum. Edition of Natural Science*, **41**, 46-53.

[48] Li, F., Wang, S., Miao, S., Yang, J., Xv, Z. and Li, W. (2015) Characteristics of Low Permeability Reservoirs and Main Controlling Factors of High Quality Reservoirs of Chang 6_3 Menber in Huaqing Area. *Journal of Jilin University. Earth Science Edition*, **45**, 1580-1588.

[49] Li, X., Liu, H., Wanyan, R., Zhang, Z., Niu, H., Liao, J., Yuan, X. and Wang, J.

(2014) "Argillaceous Parcel" Structure: A Direct Evidence of Debris Flow Origin of Deep-Water Massive Sandstone of Yanchang Formation, Upper Triassic, the Ordos Basin. *Acta Sedimentologica Sinica*, **32**, 611-622.

[50] Miramontes, E., Eggenhuisen, J.T., Jacinto, R.S., Poneti, G., Pohl, F., Normandeau, A., Campbell, D.C. and Hernández-Molina, F.J. (2020) Channel-Levee Evolution in Combined Contour Current-Turbidity Current Flows from Flume-Tank Experiments. *Geology*, **48**, 353-357. https://doi.org/10.1130/G47111.1

[51] Guo, Q., Li, Z., Yu, J. and Li, X. (2010) Meso-Neozoic Structural Evolution in the Western Margin of Ordos Basin with Respect to Uranium Ore Formation. *Uranium Geology*, **26**, 137-144.

[52] Li, S., Deng, X., Pang, J., Lv, J. and Liu, X. (2010) Relationship between Petroleum Accumulation of Mesozoic and Tectonic Movement in Ordos Basin. *Acta Sedimentologica Sinica*, **28**, 798-807.

[53] Kang, L., Ren, Z., Zhang, L., Wei, B. and Wang, W. (2020) Fracture Characteristics of Chang 6 Tight Oil Reservoir in Block Y in Ordos Basin. *Journal of Jilin University. Earth Science Edition*, **50**, 979-990.

[54] Gao, J., Zhou, L. and Feng, Q. (2018) The Characteristics and Formation Phase of Structural Fracture of the Jiyuan-Yuancheng Area in the Ordos Basin. *Journal of Geodesy and Geodynamics*, **38**, 811-817.